Modelling of Stent Deployment and Deformation in Diseased Arteries by Considering Vessel Anisotropy

A. Schiavone, L.G. Zhao
L.Zhao@lboro.ac.uk

Abstract

In this paper, finite element simulation of stent deployment was carried out using an anisotropic model for the artery, consisting of three individual tissue layers, i.e., intima, media and adventitia. Each layer was modelled as a hyperelastic anisotropic material described by the Holzapfel-Gasser-Ogden (HGO) model. The model parameters were calibrated against the experimental stress-stretch responses in both circumferential and longitudinal directions. The results showed that, at the peak pressure, stent expansion obtained using the anisotropic model was much reduced when compared to that obtained using the isotropic model. However, after deflation, the finally achieved diameter for the anisotropic model is comparable to that for the isotropic model, due to the significant reduction in recoiling for the anisotropic model. Also, the anisotropic model generated slightly higher levels of stress in the artery-plaque system than the isotropic model. For the isotropic model, the high-level stresses were found mainly on the plaque, while, for the anisotropic model, both the intima layer and the plaque experienced high-level stresses. The media and adventitia layers had lower stress levels due to their relatively softer stress-strain response in the circumferential direction as well as limited deformation. Following deployment, deformation of the stent was also modelled by applying relevant biomechanical forces, such as bending and radial compression, to the stent-artery system. The results were utilised to interpret the mechanical performance of stent after deployment.

Key words: Stent deployment; Vessel anisotropy; Finite element; Artery stenosis; Biomechanical forces.

1 Introduction

Coronary stents are essentially scaffolds, made of metallic alloys or biopolymers, used to sustain the blood vessels once expanded inside the obstructed arteries. Stents are generally deployed inside the diseased artery by means of an angioplasty balloon (except for self-expandable stents). The scaffold is placed over the balloon and expands with the balloon when this is inflated by internal pressure. This surgery procedure has minimal invasive nature and provides fast and effective solutions to patients suffering from coronary stenosis, a major cause of heart attack.

Finite element is an effective tool to simulate the process of stent expansion inside stenotic arteries, which helps to understand the insight of the biomechanical behaviour of the whole stent-artery system during the procedure. The simulations provide essential information regarding stent expansion, recoiling, dogboning and residual stresses, which can be further utilised to guide stent design and surgery procedures [1, 2, 3, 4, 5]. The artery constitutive model is an important factor for simulation of stent deployment. [6] reviewed the state of the art of development of constitutive models in the last ten years to describe the mechanical behaviour of artery tissue. It highlighted the highly nonlinear and anisotropic behaviour of the blood vessel tissue. This work also suggested that in many cases the artery behaves purely elastically and can be characterized by hyperelastic strain energy functions, including the layer specific constitutive models used to describe mechanical behaviour of arteries. However, anisotropic hyperelastic models have seldom been used to simulate expansion and deformation of stent-artery system, and existing studies are dominantly limited to the use of isotropic models.

In this paper, finite element simulation of stent deployment was carried out using an anisotropic model for the artery. In particular, the artery wall was considered to consist of three individual tissue layers, i.e., intima, media and adventitia, which are all described by the Holzapfel-Gasser-Ogden (HGO) hyperelastic anisotropic model [7, 8]. To understand the mechanical performance of stent after deployment, deformation of the stent-artery system was also modelled under relevant biomechanical forces, such as bending and radial compression, focusing on the re-distribution of local stresses and strains in the stent.

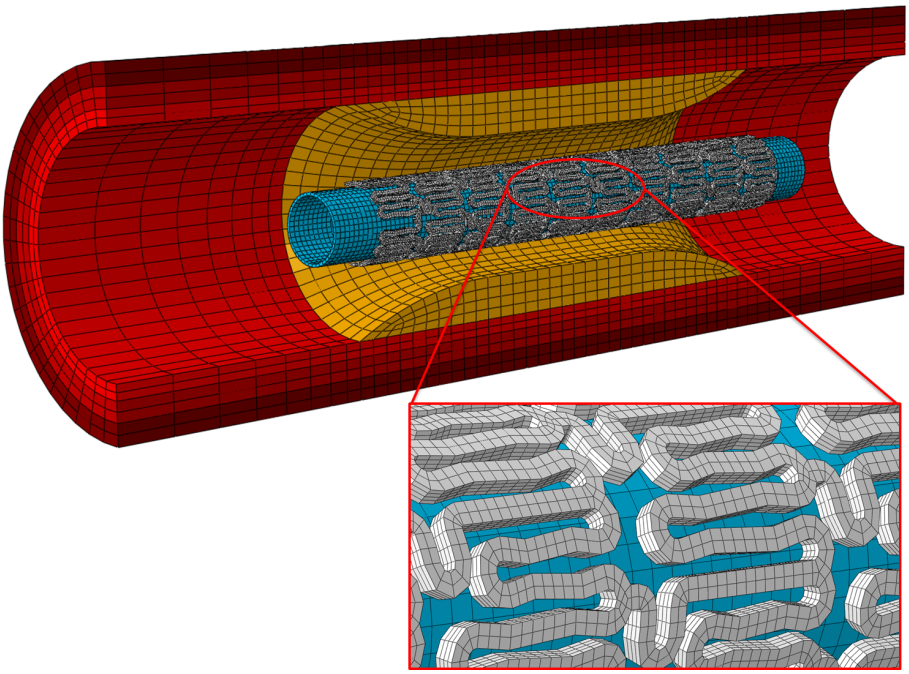

Figure 1: Finite element mesh for the Xience stent, the balloon and the stenotic artery.

2 Finite Element Model

The finite element model for the balloon-stent-artery system is shown in Figure 1. The stent used for this analysis resembles the geometry of Xience stent, one of the latest commercial stents. The stent has a crimped diameter of $1.5mm$, a length of $10mm$ and a strut thickness of $80\mu m$. The artery has a total length of $20mm$, an inner diameter of $4mm$ (healthy region) and a wall thickness of $1mm$. The artery wall is considered to have three layers, namely intima ($0.27mm$), media ($0.35mm$) and adventitia ($0.38mm$). The plaque has a length of $10mm$ and a stenosis of 40%. The balloon has a folded geometry, with a length of $12mm$.

The artery and plaque were meshed into hexahedral elements with reduced integration, which are mostly used to increase the computing efficiency and numerical convergence associated with large deformation, especially for soft tissues [9, 10]. The stent was meshed into incompatible hexahedral elements (with full integration) in order to accommodate large bending deformation of the stent strut during expansion [11]. The folded balloon was meshed using 4-node shell elements with reduced integration based on the consideration of computational efficiency.

Contacts between the stent, the artery and the balloon were defined as hard contact with a friction coefficient of 0.25 [12]. The ends of the artery and the balloon were fully constrained to remove rigid body motion. All analyses were carried out using Abaqus explicit solver [11]. The deployment simulations consisted of two steps: the inflation step ($0.1s$) in which the applied pressure increased linearly to the peak value and the deflation step ($0.1s$) in which the pressure dropped linearly to zero to allow the recoil of the artery and the stent. The pressure was applied on the inner surface of the balloon, with a peak pressure of $1.4MPa$. Following the deflation step, a third step was introduced to continue the simulations by applying bending and radial compression to the system. For bending, a displacement of $5mm$ was applied to all the nodes on the cross section at the middle of the artery, while for compression, a pressure of $0.2MPa$ was applied to the outer surface of the artery over the section where the stent was implanted.

3 Material Constitutive Behaviour

3.1. Models for stent, balloon and plaque

The Xience stent is made of Co-Cr L605 which is modelled as an elastic-plastic material with multilinear hardening segments based on the tensile stress-strain curve of the alloy given in [13]. The folded balloon was modelled as a linear elastic material with Youngs modulus of $900MPa$ and Poisson ratio of 0.3 [14]. The hypocellular plaque is described by the Ogden hyperelastic model with model parameters given in [15].

3.2. The Holzapfel-Gasser-Ogden model for artery

Experimental tests on human arteries highlighted the anisotropic behaviour of such biological tissues [7, 16]. The Holzapfel-Gasser-Ogden (HGO) anisotropic hy-

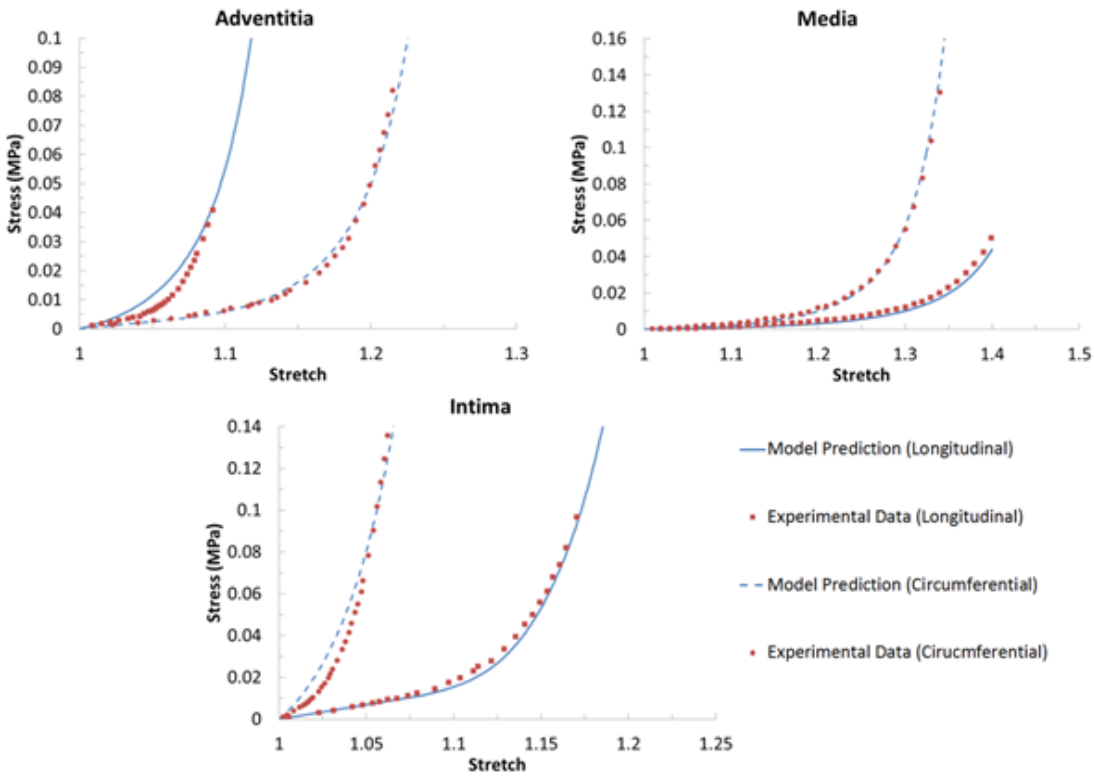

Figure 2: Anisotropic stress-stretch response of the three arterial layers, experimental results [16] versus simulations.

perelastic model [7, 8] was used, with a strain energy potential given as [11]:

$$U = C_{10}\left(\bar{I}_1 - 3\right) + \frac{k_1}{2k_2}\sum_{\alpha=1}^{N}\left\{\exp\left[k_2\left\langle\bar{E}_\alpha\right\rangle^2\right] - 1\right\} + \frac{1}{D}\left(\frac{(J^{el})^2 - 1}{2} - \ln J^{el}\right) \tag{1}$$

with

$$\bar{E}_\alpha = \kappa\left(\bar{I}_1 - 3\right) + (1 - 3\kappa)\left(\bar{I}_{4(\alpha\alpha)} - 1\right) \tag{2}$$

where $\bar{I}_1$ and $\bar{I}_2$ are the first and second stretch invariants, J is the volumetric stretch (or third stretch invariant), C_{10}, D, k_1, k_2 and κ are material parameters, and $\bar{I}_4$ is the invariant of Cauchy-Green deformation tensor. The strain-like quantity $\bar{E}$ characterizes the deformation of the fibre family and the operator $\langle\ \rangle$ stands for the Macauley bracket. The parameters of the model were calibrated to fit the experimental data given in [16]. Fitted model parameters are given in Table 1 for all three vessel layers, which give the stress-stretch responses that are in good agreement with the experimental data in both circumferential and longitudinal directions (Figure 2).

4 Results and Discussion

4.1. Stent expansion

Table 1. Values of the Holzapfel-Gasser-Ogden model parameters for the three vessel layers.

Material	ρ(kg/mm^3)	C_{10}	k_1	k_2	κ	D
Intima	1.07E-6	2.3E-2	25	1200	0.308	8.95E-7
Media	1.07E-6	1.4E-3	0.18	100	0.314	5.31E-6
Adventitia	1.07E-6	8.32E-3	4	1000	0.312	4.67E-6

The result of stent expansion is shown in Figure 3, in a comparison with those obtained from isotropic arterial model. Expansion was shown to have three stages. At the initial stage, stent deforms elastically and has a lower rate of expansion. At the second stage, plastic deformation occurs and stent seems to expand steadily, together with the artery, at a fairly constant rate. At the final stage, the rate of stent expansion starts to decrease drastically, indicating that the deformation of the stent/artery system seems to reach a saturation stage, i.e., further increase of pressure only results in very limited expansion. This is mainly due to the intrinsic deformation behaviour of the artery which reached a saturation stage of stretch, especially the intima layer (see Fig.2). Consequently, the system becomes considerably resistant to further expansion, resulting in a drastic decrease of expansion rate.

For isotropic model, stent expanded from 1.5mm to 4.8mm at the maximum pressure (1.4MPa), with an increase in diameter by more than three folds. At the peak pressure (1.4MPa), the maximum diameter achieved using the anisotropic model was only 4.1mm, which is much reduced when compared to that, i.e. 4.7mm, achieved using the isotropic model for the layers.

During deflation, recovered elastic deformation and radial pressure from the viscoelastic artery system lead to the recoil of the stent. After recoiling, the diameter was settled at 3.8mm for the anisotropic model, which is larger than that (3.7mm) computed from the isotropic model. This is due to the significant reduction in recoiling, only 8% for the anisotropic model compared to 22% for isotropic model. The achieved expansion is close to the diameter of a healthy artery.

4.2. Stress on the stent

Figure 4 compares the von Mises stress distribution on the stent for the two models following stent deployment. The stent has severe stress concentrations at the U-bends of the cell struts due to highly localised stretch. These are residual stresses which were developed due to the sustained plastic deformation. From the computed results, it appears that the anisotropic artery model increased the magnitude of the von Mises stress on the stent. For isotropic model, the magnitude of residual stress was shown to be around 778MPa, as opposed to 1384MPa for anisotropic model (Figure 4). The stress level is very significant and implies the potential risk of failure during stent employment. Consequently, optimal design of cell strut U-bends appears to be important for modern stents, which can lead to stress reduction and failure resistance. However, it should be noted that in reality, the stresses on the stents might not reach such high magnitude if the residual stresses developed during stent crimping [17, 18] are considered which shall mitigate

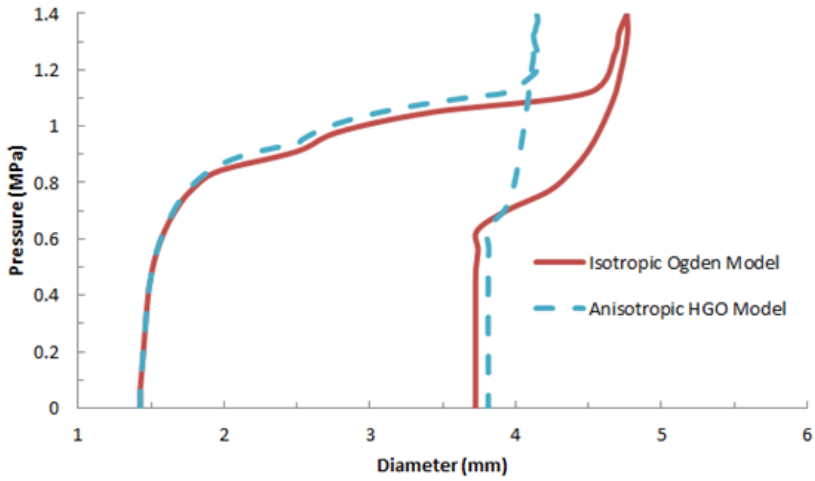

Figure 3: Comparison of diameter change against pressure for stent expansion simulated using isotropic Ogden and anisotropic HGO constitutive models for the artery.

the stresses developed during stent expansion.

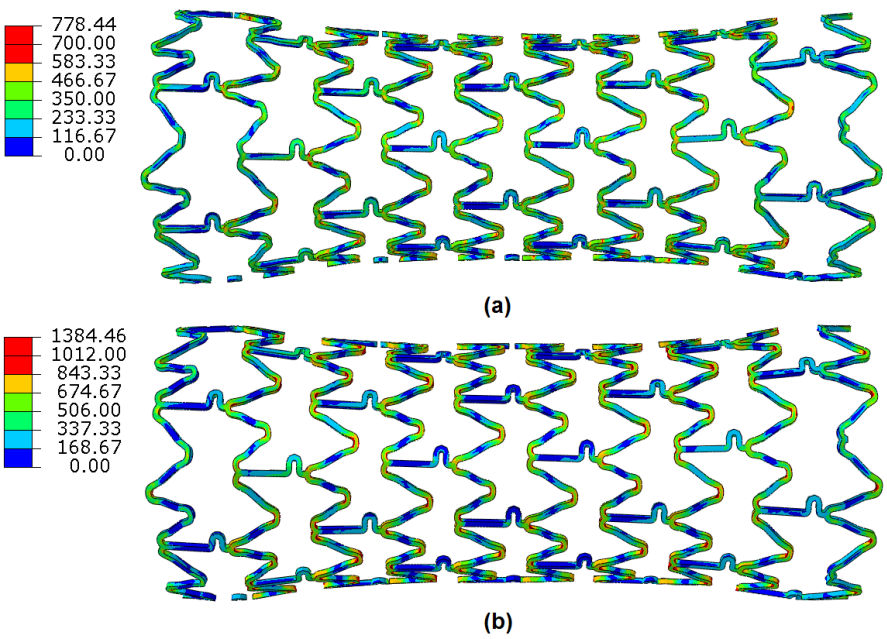

Figure 4: Stress distribution on the stent after deployment simulated using (a) isotropic Ogden and (b) anisotropic HGO constitutive models for the artery.

4.3. Stress on the artery-plaque system

The stress distribution on the artery-plaque system, after stent deployment, is compared in Figure 5, and the anisotropic model generated slightly higher levels of

stress than the isotropic model, with a maximum value of 0.70MPa (0.65MPa for isotropic model). High stress levels were mainly obtained in the intima layer as well as on the stenotic plaque surface. The media has the lowest stress level due to its soft stress-strain response in the circumferential direction. It was also noticed from our simulation, at the peak inflation pressure, the maximum von Mises stresses on the plaque-artery system were located in the intima layer of the artery with a magnitude of 7.30MPa, due to the relatively high stiffness of the intima layer as well as the severe constraint on the intima layer imposed by surrounding tissues. After deflation, the maximum stress shifted to the plaque, especially at locations where the stent and the plaque are in full contact.

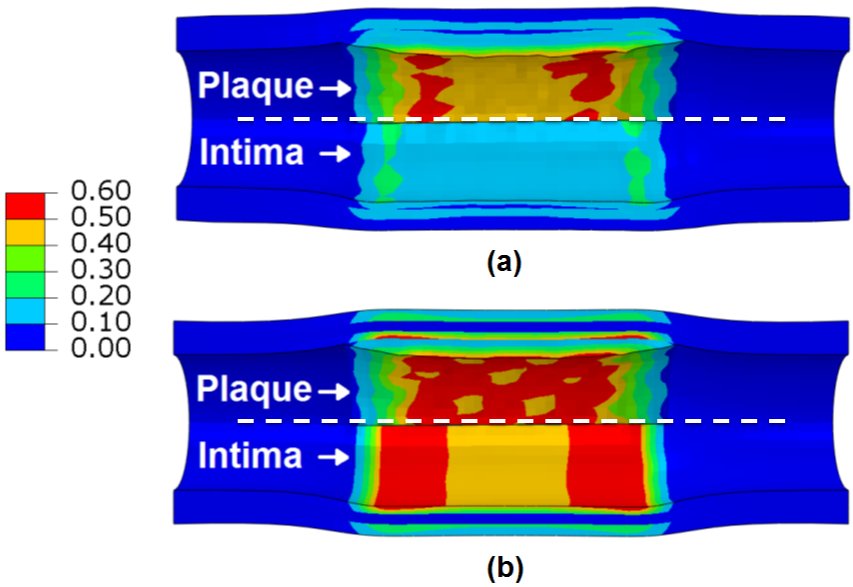

Figure 5: Stress distribution on the artery-plaque system after stent deployment simulated using (a) isotropic Ogden and (b) anisotropic HGOmodels for the artery.

4.4. Stent deformation under biomechanical forces

For the applied bending, there is hardly any change of stresses on the stent compared to the stress state after deployment. This might be because the metallic material reached a steady-state of stress-strain response in the plastic region and the stress becomes insensitive to further deformation. For radial compression, stent collapse started to occur at a pressure of about 0.1MPa, and also the right end of stent collapsed earlier than the left end due to asymmetry of the stent structure (Figure 6).

We also carried out simulations by excluding the residual stresses generated out of stent deployment. For bending, the maximum stress on the stent was found on one of the bottom longitudinal connective struts in the middle region where the system has the most severe bending deformation. The maximum stress has a value of 651MPa which is significantly less than that obtained from simulations by considering the residual stresses. Also stent collapse under compression tended to

be delayed when the residual stresses are excluded.

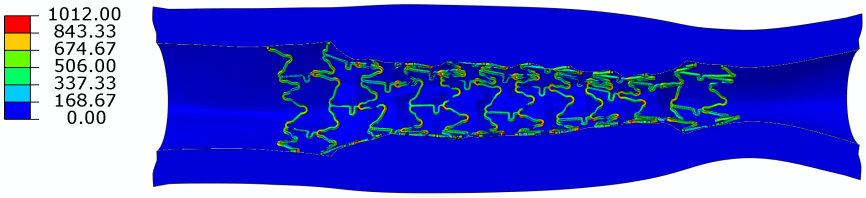

Figure 6: Stress distribution on the deformed stent-artery system at a compressive pressure of 0.2MPa.

5 Conclusions

The anisotropy of blood vessels needs to be considered in order to produce reliable and conclusive results in stent deployment simulations. It is also strongly recommended to take into account the residual stress state, generated out of stent deployment, for further mechanical performance analyses.

Acknowledgements

The research leading to these results received funding from the European Union Seventh Framework Programme (FP7/2007-2013) under grant agreement No. PIRSES-GA-2013-610547 TAMER.

References

[1] Chua SND, McDonald BJ, Hashimi MSJ (2003) Finite element simulation of stent and balloon interaction. J Mater Process Tech 143-144:591-597

[2] Pericevic I, Lally C, Toner D, Kelly DJ (2009) The influence of plaque composition on underlying arterial wall stress during stent expansion: The case for lesion-specific stents. Med Eng Phys 31:428-433

[3] Zhao S, Gu L, Froemming SR (2012) On the importance of modeling stent procedure for predicting arterial mechanics. ASME J Biomech Eng 134:121005-1

[4] Morlacchi L, Colleoni SG, Crdenes R, Chiastra C, Diez JL, Larrabide I, Migliavacca F (2013) Patient-specific simulations of stenting procedures in coronary bifurcations: Two clinical cases. Med Eng Phys 35:1272-1281

[5] Schiavone, A., Zhao, L.G., Abdel-Wahab, A.A., 2014. Effects of material, coating, design and plaque composition on stent deployment inside a stenotic arteryFinite element simulation. Mater Sci Eng C 42, 479-488

[6] Holzapfel GA, Ogden RW (2010) Constitutive modeling of arteries. Proc R Soc Ser A 466:1551-1597

[7] Holzapfel GA, Gasser TC, Ogden RW (2000) A new constitutive framework for arterial wall mechanics and a comparative study of material models. J Elasticity Phys Sci Solids 61:1-48.

[8] Gasser TC, Ogden RW, Holzapfel GA (2006) Hyperelastic modelling of arterial layers with distributed collagen fibre orientations. J R Soc Interface 6:15-35

[9] Mortier P, De Beule M, Van Loo D, Verhegghe B, Verdonck P (2009) Finite element analysis of side branch access during bifurcation stenting. Med Eng Phys 31:434440

[10] Zahedmanesh H, Kelly DJ, Lally C (2010) Simulation of a balloon expandable stent in a realistic coronary artery - Determination of the optimum modelling strategy. J Biomech 43:2126-2132

[11] ABAQUS (2014) Version 6.13, Dassault Systmes, Vlizy-Villacoublay, France.

[12] Ju F, Xia Z, Sasaki K (2008) On the finite element modelling of balloon-expandable stents. J Mech Behav Biomed Mater 1:86-95

[13] Medtronic Technical Bulletin (2003) Advantages of cobalt alloy for coronary stents.

[14] Gervaso F, Capelli C, Petrini L, Lattanzio S, Di Virgilio L, Migliavacca F (2008) On the effects of different strategies in modelling balloon-expandable stenting by means of nite element method. J Biomech 41:1206-1212

[15] Zahedmanesh H, Lally C (2009) Determination of the influence of stent strut thickness using the finite element method: implications for vascular injury and in-stent restenosis. Med Biol Eng Comput 47:385-393

[16] Holzapfel GA, Sommer G, Gasser CT, Regitnig P (2005) Determination of layer-specific mechanical properties of human coronary arteries with nonatherosclerotic intimal thickening and related constitutive modelling. Am J Phisiol - Heart C, 289:H2048-H2058

[17] Mäller D, Reimers W, Pyzalla A, Fischer A (2001) Residual stresses in coronary artery stents. J J Biomed Mater Res 58:6974.

[18] Kleinstreuer C, Li Z, Basciano CA, Seelecke S, Farber MA (2008) Computational mechanics of Nitinol stent grafts. J Biomech 41:23702378.

A. Schiavone & L.G. Zhao, Wolfson School of Mechanical and Manufacturing Engineering, Loughborough University, UK